Mining Science, vol. 31, 2024, 81–101

www.miningscience.pwr.edu.pl

Mining Science

(Previously Prace Naukowe Instytutu Gornictwa Politechniki Wroclawskiej, ISSN 0370-0798)

ISSN 2300-9586 (print)
ISSN 2353-5423 (online)

Received January 24, 2024; Reviewed; Accepted August 25, 2024

OPEN-PIT OVERBURDEN DUMP CHARACTERIZATION USING DIGITAL IMAGE PROCESSING TECHNIQUE

Radhakanta KONER*, Amit KUMAR MANKAR,
Kapoor CHAND

Department of Mining Engineering, Indian Institute of Technology (Indian School of Mines), Dhanbad 826004, Jharkhand, India

Abstract: The safety of the open-pit overburden dump slope largely depends on the geomaterial size and shape. The shape of these geomaterials contributes to their shear resistance against sliding. The present investigation proposed a method to characterize the geomaterial using the digital image processing technique. The resources invested in this work are a simple digital camera and a computational toolbox. The system estimates the size distribution of geomaterial. The study also proposed a methodology for reconstructing the 3D geometry of the mine dump from the images. The advantage of the method is a low-cost, quick assessment of the dump geomaterial, and outcomes can easily be used in a numerical toolbox. The study was conducted in Barakar Valley Coalfields, West Bengal, India. The geomaterials above 4 mm sizes are considered in this work. The results matched the mechanical sieving output of the particle size distribution curve.

Keywords: *overburden dump, geomaterial, digital image processing, particle size distribution, 3D reconstruction*

1. INTRODUCTION

In India, the contribution of surface mining to coal production is over 90 percent (Mishra et al. 2024). Surface mining generates the vast amount of overburden (Chand and Koner 2024) and this overburden material are dumped internally or externally based on area of requirement. Open-pit dump slope is an artificial structure built on this

* Corresponding author: rkoner@iitism.ac.in (R. Koner)

doi: 10.37190/msc243105

earth to store and manage mine waste overburden geomaterials. The planning and design of dump slopes require understanding the overburden geomaterial characteristics (Chand and Koner 2016). Traditional drilling and blasting are adopted to remove overburden in the open-pit mine; the performance of this operation influences the size and shape of the geomaterial produced. In a recent study showed that the stability of the dump slope largely depends on the alignment of the dumping sequence and its orientation (Koner 2021). Storage of higher-size overburden geomaterials at the bottom and sequentially heightening dump slopes with medium and smaller sizes could have been the best way to manage the stability. The waste geomaterials are randomly deposited at the internal or external mine dump, making it a heterogeneous assembly. In the engineering investigation, the cumulative and blending mixture of rock and soil in the dump slope was compromised, and associated errors were ingrained in the stability analysis. Reports of slope failure are only available when the factor of safety is greater than 1. So, we needed to characterize dump geomaterials using a non-evasive method for a quick and exhaustive onsite assessment.

Overburden slopes are composed of rock fragments and loose soil, which are densely packed. Collecting geomaterial samples from the slope is complex, particularly far inside the assembly. In the physicomechanical characterization of dump geomaterials, size, shape, and texture are necessary (Xu et al. 2008). The quantitative distribution of size and shape in the blasted overburden in open-pit mines indicates the performance and efficiency of the total mining production cycle (Sereshki et al. 2016). Rock particles size, shape, and texture in quarry production must fit the customers' requirements, for example, highway, railway construction companies, building industries, etc. (Karakus et al. 2010).

Characterizing the dump geomaterial is the primary goal of geotechnical engineers. The geotechnical data obtained from various tests is highly subjective, and variability in dump geomaterial conditions increases over time and space. Different testing methods exist to characterize and classify dump geomaterial, and one of the most preliminary methods is determining grain size distribution. It assumes that dump geomaterials with similar sizes and shapes have uniform properties. The laboratory's estimation of particle size distribution involves mechanical sieving for coarse-grained geomaterials. Hydrometer analysis was followed for fine-grained geomaterials. A typical grain size distribution curve obtained from sieving is shown in Fig. 1.

A single linear dimension, which represents the minimum square sieve aperture through which the particle has just passed, is used to characterize the particle size in sieve analysis (Ghalib and Hryciw 1999). The particles shape is a determining factor in the results of sieving (Mora and Kwan 2000; Mora et al. 1998; Kwan et al. 1999). Mechanical sieving involves passing the geomaterial through a set of standard sieves. The weight of geomaterials retained on each sieve set is measured and plotted as a passing percentage against the particle size. There are several limitations to this method, which are outlined below.

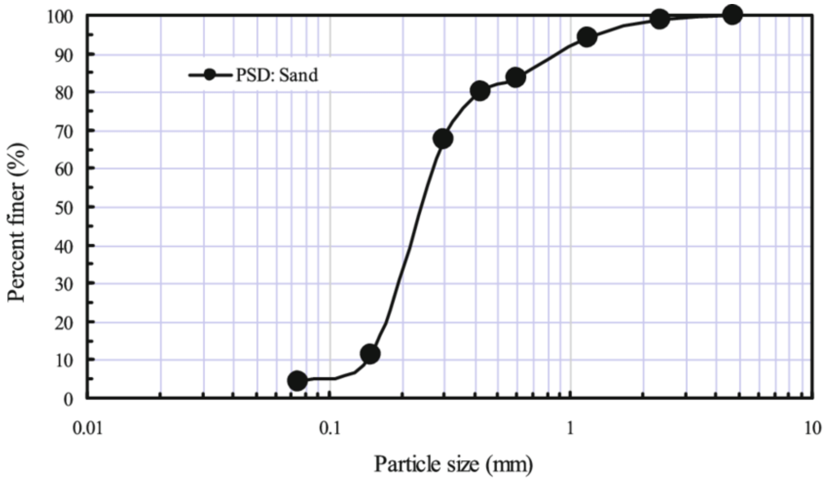

Fig. 1. Grain size distribution curve (Mir and Ashraf 2019)

Geomaterial properties depend not only on the grain size distribution of particles but also on other factors like mineral constituents, elemental structural arrangements, geological history, etc. The sieving apparatus also require maintenance at regular interval. On repeated use, the sieve openings get distorted and give erroneous results. More importantly, sieve analysis does not necessarily measure the particle diameter in the conventional sense. Geomaterial particles are three-dimensional, and particle size is determined by sieving, which captures the intermediate dimension.

In the case of fine-grained geomaterials, sieve analysis is not appropriate. The physical properties of clay, such as plasticity, control the mechanical behaviour rather than particle size distribution. Hydrometer analysis is based on the sedimentation principle and Stoke's law. The grain size is calculated from the sedimentation distance of geomaterial particles. The limitations of hydrometer analysis are described here.

It assumes that all geomaterial particles are spherical. However, clay and silt particles are plate-like and flaky. Overburden geomaterial contains particles with different mineral constituents; thus, the specific gravity cannot be characterized using an average value. The test assumes that the geomaterial particles are separated from one another. Although a dispersing agent is added to the geomaterial-water suspension to ensure the validity of this assumption, some particles flocculate and settle more rapidly than individual particles. The test also assumes that the particles do not interact with one another. However, this may not necessarily be true if the concentration of the geomaterial-water suspension is high.

Automation is gaining much importance with the advancement of technology and the use of computers. It not only expedites the process, but also produces more objective results. This work uses automation procedures to determine the grain size distribution of waste overburden geomaterial.

There are many characterisation methods (Gee and Or 2002), and the latest digital image processing technique uses a simple digital camera. Image analysis is a beneficial method for determining the particle-size distribution of soils. It offers advantages such as reduced testing time, lower expenses, and improved working environment (Akbulut et al. 2011). Several studies have employed image analysis to determine the size distribution, particle shape, and surface roughness of aggregates in two and three dimensions (Taylor 2002; Maerz 2004; Fernlund 2005a; 2005b; 2005c; Tutumluer et al. 2005; Lira and Pina 2007; Maerz and M. Lusher 2001).

Overburden dump 2D images have some particular characteristics compared to other images. Under the front lighting illumination condition, which is the typical case, geomaterial particle images have the following features: (1) uneven background and foreground for which a simple threshold algorithm cannot be applied to segment the images, (2) each geomaterial fragment possesses textured surface and multiple faces, which often causes an over-segmentation problem, (3) geomaterial fragments overlap each other, resulting some part hidden underneath, and incompleteness of the boundaries of geomaterial particles, (4) clubbing of geomaterial fragments form a large cluster, (5) rain, snow, or fantastic soil material makes geomaterial assembly as a clump in the images. This work developed an automated algorithm to identify and measure overburden geomaterial fragments using intensity images of the surface of the overburden dump.

The precise volume of the mine overburden dump is often compromised with the traditional surveying techniques used in the fields. An accurate slope profile (geometry) is required for structural stability analysis. Surface mine demands a fast but straightforward approach that will give a reasonable estimation of the 3D surface of the overburden dump vis-à-vis that would be useful for numerical analysis to assess the stability. The image processing technique has an answer to this particular problem.

So, this work will essentially concentrate on image processing techniques for characterizing dump geomaterial. 3D mine dump profile will be reconstructed from camera images taken at different angles from different sides of the dump in broad daylight in a mine in the Barakar Valley Coalfields, India.

2. MATERIALS AND METHODOLOGY

The study uses a SONY Cyber-Shot DSC-HX400V camera for collecting 2D images of the mine dump and overburden geomaterial. A mine of Barakar Valley Coalfields was selected for this study. The mine area is bounded by the rural areas of Jamuria CD Block on the north, Kenda Area and Kajora Area on the east, Bankura district across the Damodar on the south, and Satgram Area and Sripur Area on the west. The mine area is located around 23.645711°N and 87.117422°E.

Samples were collected and kept at the testing facility of our institute. Geotechnical tests were conducted, and the grain size distribution curve profile obtained from image analysis was compared. The study used MATLAB (Hunt et al. 2001) and MESHLAB (Hunt et al. 2008) for the entire computation.

The image processing for the geomaterial characterization starts with pattern recognition of dump geomaterial particles and fragments, i.e., image segmentation. Segmentations are of two types; the first is segmentation based on grey levels (called Image Binarization). A grey-level image is processed and converted into a binary image. Segmentation is based on particle shapes in a binary image; overlapping particles in contact will split, and over-segmented particles will be merged based on prior knowledge, such as shape and size, etc.

Image segmentation divides an input image into distinct regions of uniform properties, such as intensity, colour, and texture (Vangla et al. 2014). The methods are often effectively used in many application areas of image processing. Segmentation algorithms for monochrome (grey-level) images are based on two fundamental grey-level values: similarity and discontinuity. The principal approaches in the first category are based on thresholding, region growing, and region splitting and merging. In the second category, the method is partitioning an image based on abrupt changes in the grey level. This category's principal areas of interest are detecting isolated points, lines, and edges in a snap. The choice of segmentation on dump geomaterial based on the similarity or discontinuity of the grey level values depends on developed sub-algorithms and applications.

Edge detection is a developed segmentation algorithm used in this framework (Lu et al. 1988). The edge detection process has followed the flow chart shown in Fig. 2.

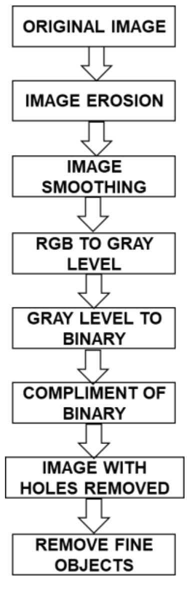

Fig. 2. Flow chart of edge detection process

The process starts with laying the geomaterial on a plane table. The geomaterial particles were placed so that no particle touched/overlapped with any other particle (see Fig. 3). The camera was mounted perpendicular to the plane, and an image was acquired. As mentioned in the process, this image is input (see Fig. 2). Holes were removed from the processed image to detect the edge.

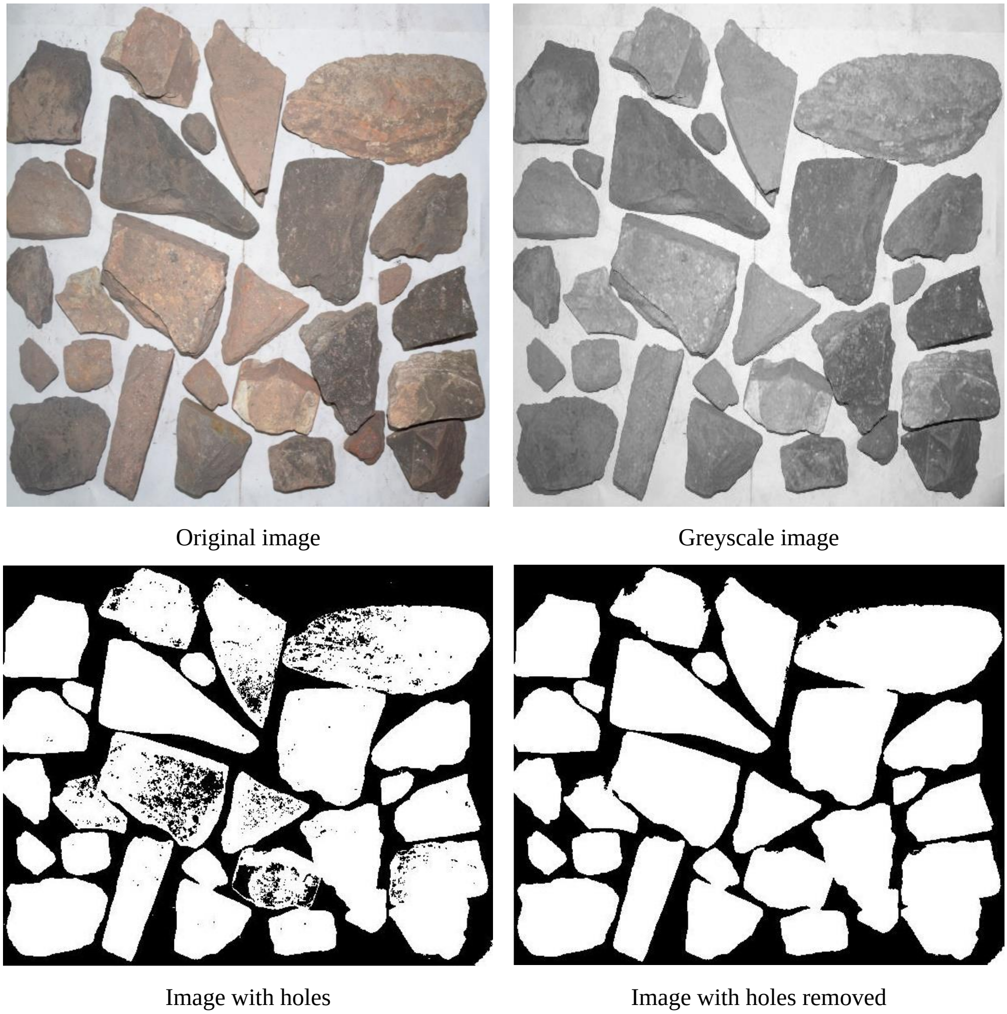

Fig. 3. Laboratory scale experiment on edge detection process

The split algorithm consists of three different processes order, namely (1) detection of holes inside an object, (2) multiple contacts in between particles, (3) two or three particles in contact. All three processes are essential for the performance of this algorithm. A watershed transform algorithm has been used for this process. The Watershed Transform combines elements based on discontinuity and similarity methods. The initial development was with greyscale images (Rubin 2004); now, this transform has been modified and extended to a computationally efficient form and applied to colour images. This method has been used to detect dump geomaterial grains or particles. The result of the developed process is shown in Fig. 4, revealing the number of particles captured.

The advantages are: (a) The resulting boundaries are closed and connected. Traditional edge-based techniques often form disconnected boundaries that need post-processing to produce closed regions, (b) The edges of the resulting areas always correspond to contours similar to objects. This contrasts with split and merge methods where the first splitting is often simple regular sectioning of the image, leading to sometimes inconsistent results, (c) The union of all regions.

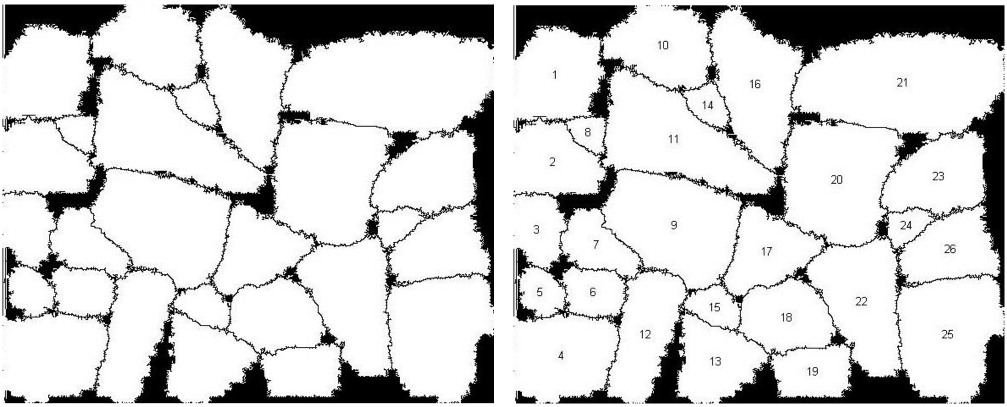

Split image Numbering of objects

Fig. 4. Laboratory scale experiment on splitting and numbering of dump geomaterial particles

The proposed method works well for the sparsely distributed geomaterial particle and the overlapping condition.

3. RESULT AND DISCUSSION

The methodology applies to random 2D images of overburden dump geomaterial aggregate (see Fig. 5). The picture (see Fig. 5) was segmented to calculate the area of individual particles from the binary image using the code. The code works and detects the particle individually and distinctly, as shown in the segmented image (see Fig. 6).

Fig. 5. Mine dump geomaterial aggregate

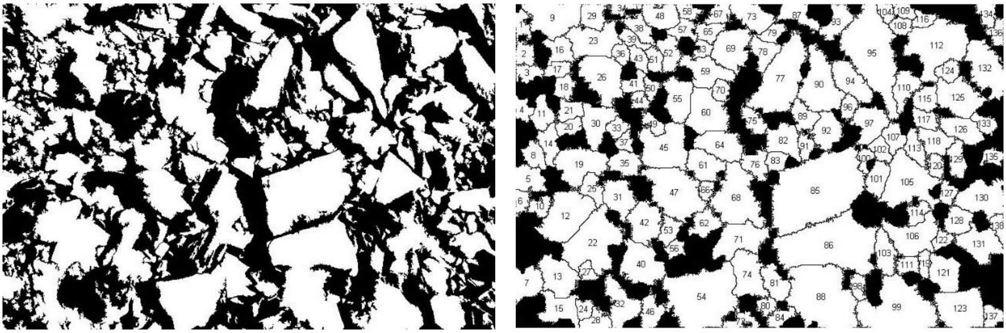

Image with touching particles Image with splitter and numbering

Fig. 6. Segmented mine dump geomaterial aggregate

The code’s effectiveness is that segmented images capture particles of different size ranges except for the finer ones, making it a handy and portable tool for reconnaissance surveys in the overburdened dumpsite.

Original image Entropy filtered image

Fig. 7. Entropy filtering for sparsely placed rock particles (Entropy = 0.9334)

Image entropy is a quantity that describes the "business" of an image, i.e., the amount of information that a compression algorithm must code. Low entropy images containing a large amount of black sky have very little contrast and large runs of pixels with the same or similar DN values. A perfectly flat image will have an entropy of zero. Consequently, they can be compressed to a relatively small size. On the other hand, high entropy images, such as an image of heavily cratered areas on the moon, have a great deal of contrast from one pixel to the next and consequently cannot be compressed as much as low entropy images. The entropy is found in the range of 0.9334, shown in Fig. 7. So it indicates these image does not require further processing for compression.

In statistics, the standard deviation (SD) is a measure used to quantify the variation or dispersion of a set of data values. A low standard deviation indicates that the data points are close to the set's mean (the expected value). In contrast, a high standard deviation indicates that the data points are spread over a broader range of values. The standard deviation filter estimates the standard deviation and assigns that value to the centre pixel in the processed image. It can measure the variability, so it is used in edge sharpening, as the intensity level changes at the edge of the picture by a considerable value. The SD filter analysis is described in Fig. 8.

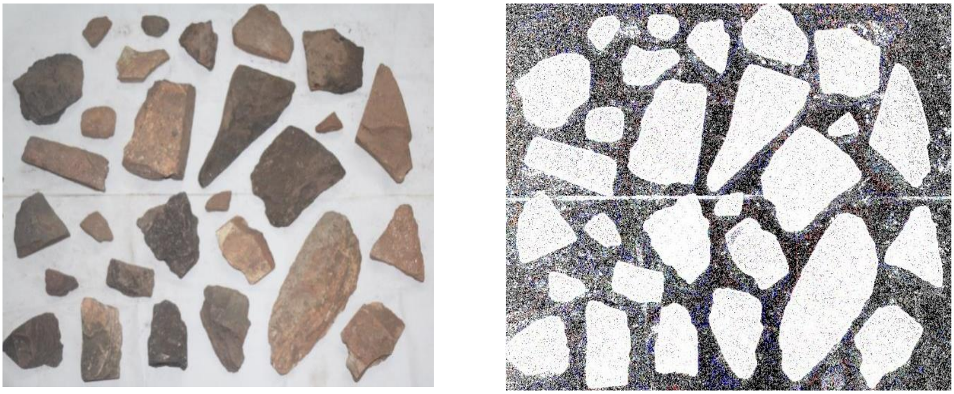

Original image Filtered image

Fig. 8. Standard deviation filtration for sparsely placed rock particles (SD = 1.6059)

3.1. MINE DUMP MATERIAL CHARACTERIZATION

The image shown in Fig. 9 represents a pile of loose soil aggregate. The geomaterial was placed at the surface mine's top of the internal overburden dump. Initially, the image was segmented using the developed method. The resulting segmentation is shown in Fig. 10.

Fig. 9. Loose soil aggregate of the dump geomaterial
at Barakar Valley Coalfields

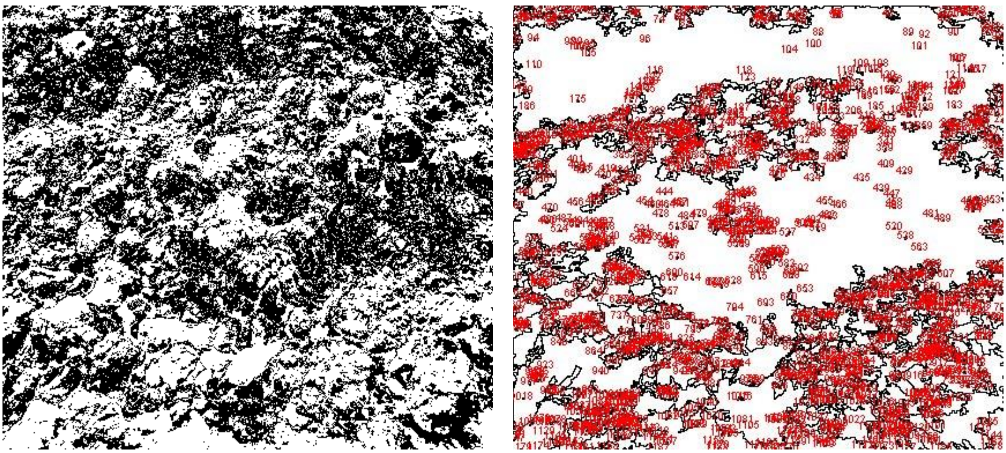

Thresholding Point detection

Fig. 10. Dump geomaterial after thresholding

Laboratory Sieve analysis was conducted as per ASTM standards. Samples weighing 500 and 152 g were taken respectively and sieved through sieve sizes of 4.75, 5.6, 10, and 12.5 mm. Only gravel was taken, i.e., a sample that retains (>=50%) on a 4.75 mm and above sieve. A Sieve shaker was used for sieve analysis and sieved for 10 min (see the setup in Fig. 11).

Fig. 11. Sieve Shaker set up for the present investigation

Soil samples weighing 152 grams were placed on white chart paper. High-resolution images of the soil sample were taken with a camera. A ruler was placed at the bottom of the model, which was included in the picture. We have tried to put the light from all sides to avoid shadow effects. The particles were separated from each other to avoid overlapping.

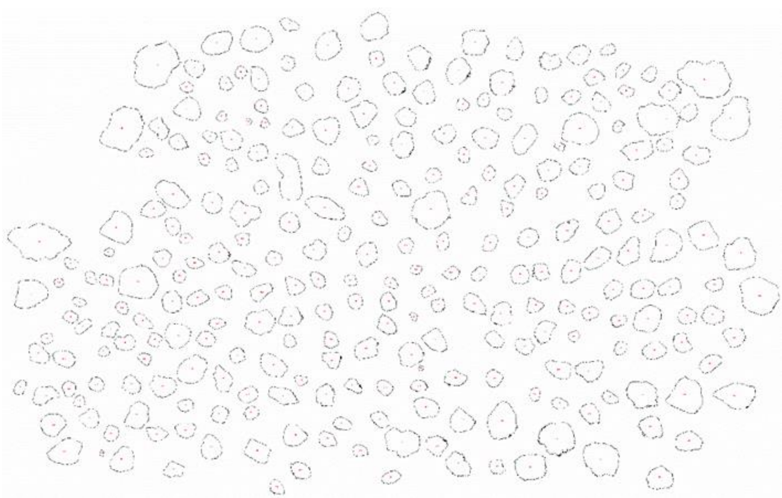

Fig. 12. Detected 262 particles of gravel sample

After importing the image in *ImageJ* (Abràmoff et al. 2004), the scale of the image was set. The scale was developed to the mm level. Two ends of the scale sizing 10mm were selected and calibrated accordingly. We then generate the image showing the soil sample's total particles, diameter, and area. A total of 262 particles are detected, which is highly accurate (Fig. 12).

Case 1

Initially, we took 500 g of gravel sample (50% or more particles retained in the 4.75 mm sieve and above). Then we sieved the geomaterial particles with the help of a sieve shaker. After that, we weighed the soil sample retained on various sieves, calculated the percentage finer, and plotted a grain size distribution graph.

We took a sample weighing 152 g from the above model and found the grain size distribution using the image processing technique. Here the categorisation of particles is done concerning the number of particles, whereas in sieve analysis, it was done by taking the mass of the soil sample.

The size distribution curve determined by image analysis differs from the sieve analysis (see Fig. 13). This difference can be mainly due to the shadow effects of the particles, the shape of the particles is assumed wrong, or maybe since a small portion of the soil was taken (in image analysis), there is a possibility that the small amount of soil contains particles of the mostly same size. There is a constant gap between the two plots, and the percentage more delicate than 12.5 mm increases in the case of image analysis. In the following point, we will see the graph's trend when the sample's exact weight is considered for both the sieve and image analysis.

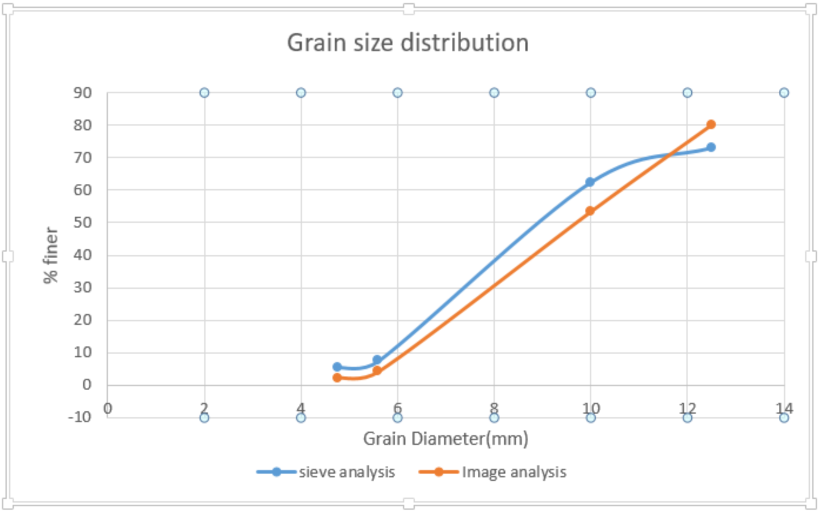

Fig. 13. Grain size distribution from the sieve and image analysis
when a small sample (152 g) was taken for image processing from 500 g sample

Case 2

In this case, we consider the entire sample, i.e., 152 g. of soil sample used for image processing in sieve analysis (see Fig. 14). We see that both the graphs almost coincide. Initially, for particles of 4.75 mm, both the lines almost coincide, continue for some time, and again part ways by a small gap that ends up very close.

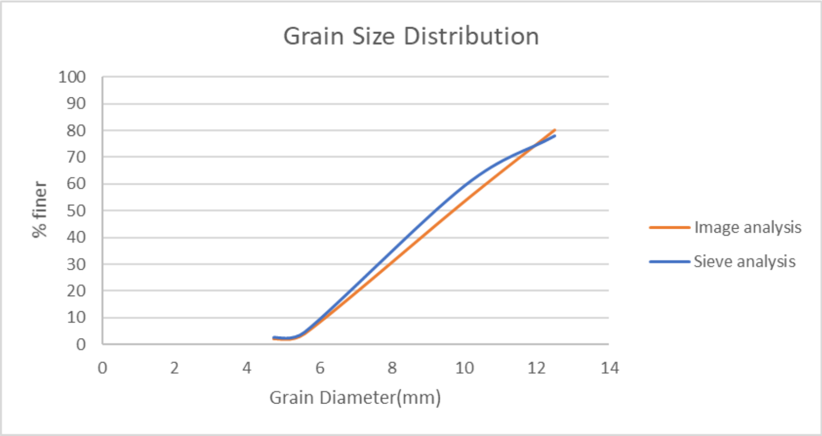

Fig. 14. Grain size distribution from the sieve and image analysis when the entire sample (152 g) was taken for image processing

So, from this, we can say that Case 2 gave a better result than Case 1. When we considered the entire sample for sieve analysis, the accuracy increased suddenly. This gives us an idea about grain size distribution using image processing techniques. This reduces time and workforce and is also cost-effective.

3.2. 3D RECONSTRUCTION OF MINE DUMP

We have captured hundreds of overburden dump images at the mine site. The image was taken at a distance all-round the dump. The weather was a bright sunny day.

Two image pairs of adjacent viewpoints were taken of the mine dump and undistorted to remove any lens distortions. Lens distortions can affect the accuracy of the final reconstruction. The image was also converted to grayscale to perform various image processing techniques. The process followed is summarized in Fig. 15.

Good features from the image pairs were tracked. Here we use the SURF algorithm for feature detection and matching. The SURF is a robust local feature detector method (Bay et al. 2006), which is inspired by SIFT but works differently. SURF characteristics are extracted using a Hessian Matrix (Neubeck and Van Gool 2006). Increasing the NumOctaves (Number of Octaves) helps us to detect large-scale features in high-resolution images. It is an integer scalar greater than or equal to 1. Increasing this value helps us see more giant blobs. A Region of Interest (ROI) was also specified, which helps detect the corners within a particular area of a size determined by width and height. The "Upright" feature's function helped us improve the matching as long as the camera motion involves little or no in-plane rotation.

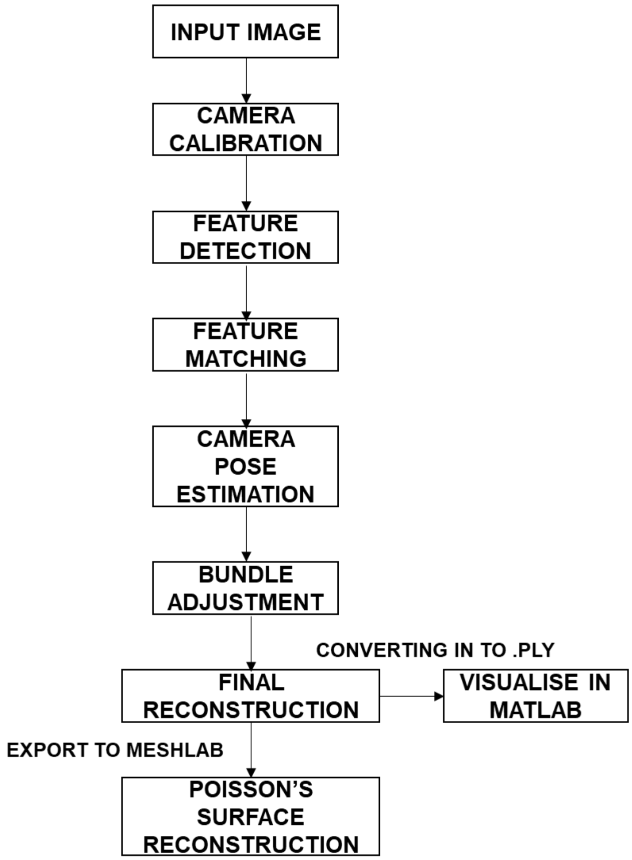

Fig. 15. Flow chart of 3D reconstruction for mine dump

The sample image pair has shown in Fig. 16. The undisturbed couple of images acquired by the camera and used as input in the present algorithm are shown in Fig. 17. The image pairs are overlapped (see Fig. 18), the point correspondence is found, and the features are matched. From the images, a lot of wrong-matched points have been seen. Those points were eliminated using the RANSAC algorithm (Fischler and Bolles 1981). It helps select a random subset of data, and the model for the selected data was found. All the data was tested against the model, and the inliers were determined based on some threshold. If the distance between the given data and model is less than the threshold, it is considered an inlier and taken as a correctly matched feature.

Fig. 16. Two image pairs of the dump

Fig. 17. Undistorted image

The point matches were stored in a particular variable. The camera pose of the current view concerning the previous picture was estimated. The carriage is computed up to scale, meaning that the distance between the cameras in the last idea and the current view is set to 1, corrected by bundle adjustment.

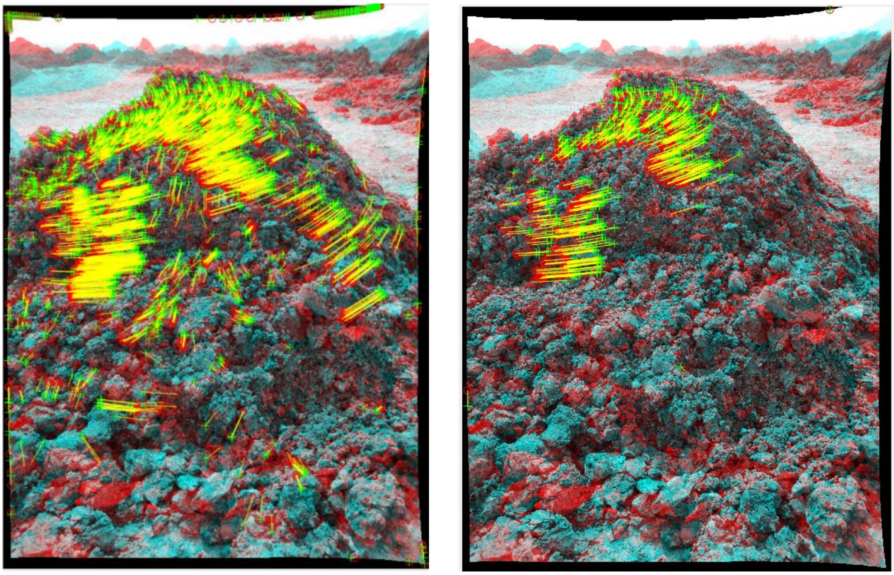

(a) (b)

Fig. 18. Overburden heap image pairs showing feature matches:
(a) all matched features, and (b) only the correct matches

Every camera poses estimation from one view to the next and contains errors. The errors arise from images' imprecise point localization, noisy matches, and inaccurate calibration. These errors accumulate as the number of views increases, an effect known as drift. Refining camera poses, and 3-D point locations are one way to reduce the importance. The nonlinear optimization algorithm, implemented by the bundle Adjustment function, was used for the refinement. The bundles of light rays that are leaving the 3D feature and converging on each camera center are referred to as bundle block adjustments. These changes are made in order to achieve the best possible results with regard to both the feature and camera placements (Triggs et al. 2002).

3.3. DENSE RECONSTRUCTION

Again, the above operations were performed through all the images (see Fig. 19). This time a dense set of corners were detected and tracked across all views. The size of the points in the point cloud was given, and the re-projection error was removed.

The importance of three-dimensional reconstruction comes from computer algorithms' inability to make significant inferences regarding our three-dimensional world without input from all spatial dimensions. Commonly, we fill this gap in the algorithm ability using tricks and manipulation based on our understanding of the space as humans rather than the computer seeing in 3D.

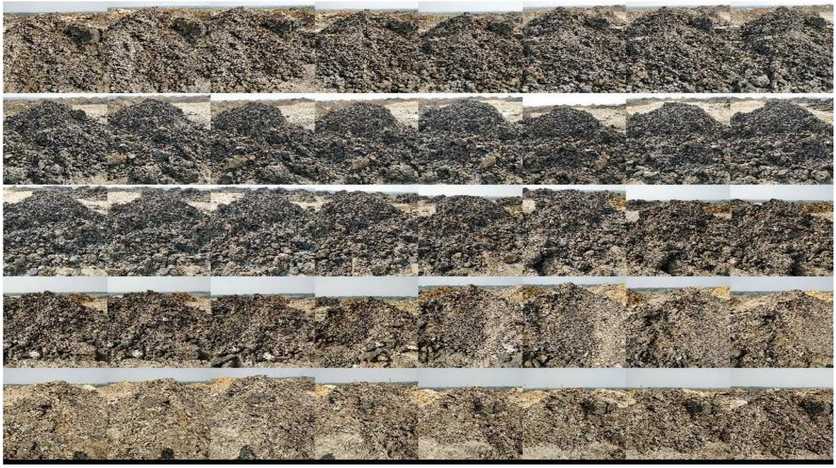

Fig. 19. Images of the mine dump from all viewpoints

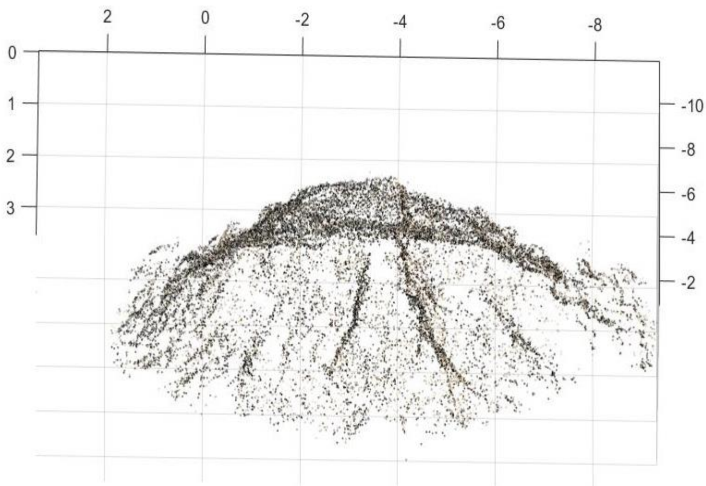

Fig. 20. Point cloud generated after processing

3.4. MESH GENERATION

The 3-D reconstruction (see Fig. 20) method is incomplete unless we create a surface out of the point cloud. A mesh was created from the point cloud using Poisson Surface Reconstruction (Kazhdan et al. 2006) in Fig. 21. Surface reconstruction can be accomplished by a variety of well-known techniques, including Poisson Surface Reconstruction (Kazhdan and Hoppe 2013), Delaunay Triangulation (Attene and Spagnuolo 2000), and more techniques, but Poisson surface reconstruction is a prevalent method for reconstructing surfaces because to its exceptional stability and reliability (Berger et al. 2014). Creating a mesh is very much important as we can do various measurements on the object. The volume and area of the mine dump can be calculated.

A section from the solid object has also been generated to get the 2D profile of the surface in Fig. 22. The 2D area can be cut in various intervals per the numerical stability analysis requirement following this algorithm.

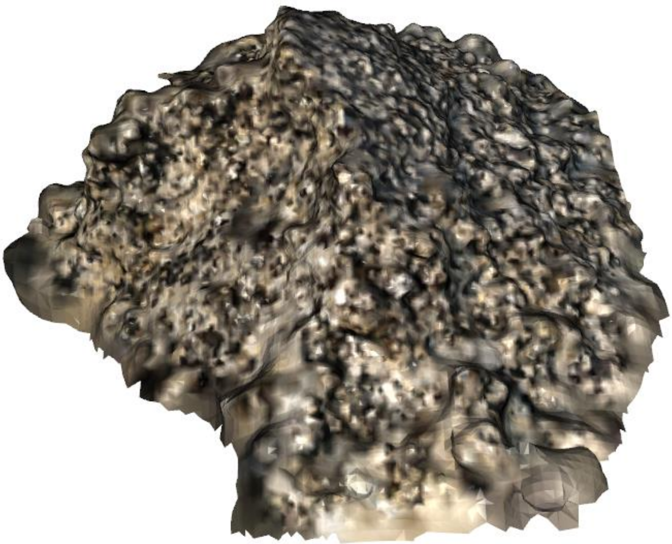

Fig. 21. Mesh surface generated using Poisson surface reconstruction

(a) (b)

Fig. 22. 3D reconstructed model of overburden heap: (a) final mesh surface of the 3D reconstructed model, and (b) a cross-sectional view of the 3D reconstructed model showing the 2D profile

4. CONCLUSIONS

The method described above is a non-contact automated geomaterial characterization technique. The method may be used for extensive overburden dump geomaterial size characterization in the field. So, it is an alternative to the traditional sieving analysis, which requires much time for sample preparation.

The significant advantage of the proposed method is that there is no upper bound for the rock particle size composed in the overburden dumps. This algorithm may use as a decision-making toolbox for mine management to quickly assess geomaterial size ranges in the mine dump.

The 3D surface reconstruction of the mine dump is another essential aspect of the present study. This method has a significant advantage over the conventional surveying process in predicting accurate surface topography of the mine dump – the numerical analysis requires precise geometry to estimate stability conditions. Thereby present method proposed an excellent alternative tool for this very purpose.

REFERENCES

ABRÀMOFF M.D., MAGALHÃES P.J., and RAM S.J., 2004, *Image processing with ImageJ*, Biophotonics International, Vol. 11, No. 7, pp. 36–42.

AKBULUT S., ARASAN S., and HASILOGLU A.S., 2011, *Effect of particle size and shape on the grain--size distribution using image analysis*, *International Journal of Civil and Structural Engineering*, Vol. 1, No. 4, pp. 968–985, doi: 10.6088/ijcser.00202010083.

ATTENE M. and SPAGNUOLO M., 2000, *Automatic surface reconstruction from point sets in space*, Computer Graphics Forum, Vol. 19, No. 3, pp. 457–465.

BAY H., TUYTELAARS T., and VAN GOOL L., 2006, *SURF: Speeded Up Robust Features*, ECCV 2006, Lecture Notes in Computer Science, Vol. 3951, pp. 404–417.

BERGER M. et al., 2014, *State of the Art in Surface Reconstruction from Point Clouds*, Annual Conference of the European Association for Computer Graphics, Eurographics.

CHAND K. and KONER R., 2024, *Mine Active Internal Dump Susceptible Zone Identification using MMO Technique*, Journal of Mines, Metals and Fuels, pp. 165–177, Apr., doi: 10.18311/jmmf/2024/35719.

CIGNONI P., CALLIERI M., CORSINI M., DELLEPIANE M., GANOVELLI F., and RANZUGLIA G., 2008, *MeshLab: an Open-Source Mesh Processing Tool*, *Eurographics Italian chapter conference*, pp. 129–136.

FERNLUND J.M.R., 2005a, *Image analysis method for determining 3-D size distribution of coarse aggregates*, Bulletin of Engineering Geology and the Environment, Vol. 64, No. 2, pp. 159–166, Jun., doi: 10.1007/s10064-004-0251-8.

FERNLUND J.M.R., 2005b, *Image analysis method for determining 3-D shape of coarse aggregate*, Cem. Concr. Res., Vol. 35, No. 8, pp. 1629–1637, Aug., doi: 10.1016/j.cemconres.2004.11.017.

FERNLUND J.M.R., 2005c, *3-D image analysis size and shape method applied to the evaluation of the Los Angeles test*, Eng. Geol., Vol. 77, No. 1–2, pp. 57–67, Feb., doi: 10.1016/j.enggeo.2004.08.002.

FISCHLER M.A. and BOLLES R.C., 1981, *Random sample consensus: a paradigm for model fitting with applications to image analysis and automated cartography*, Commun. ACM, Vol. 24, No. 6, pp. 381–395.

GEE G.W. and OR D., 2002, *Particle-Size Analysis*, [in:] *Methods of soil analysis: Part 4. Physical methods*, Vol. 5, pp. 255–293.

GHALIB A.M. and HRYCIW R.D., 1999, *Soil particle size distribution by mosaic imaging and watershed analysis*, Journal of Computing in Civil Engineering, Vol. 13, No. 2, pp. 80–87.

HUNT B.R., LIPSMAN R.L., and ROSENBERG J.M., 2001, *A Guide to MATLAB*, doi: 10.1017/cbo9781139164801.

JIE XU W., QI YUE Z., and LIN HU R., 2008, *Study on the mesostructure and mesomechanical characteristics of the soil-rock mixture using digital image processing based finite element method*, International Journal of Rock Mechanics and Mining Sciences, Vol. 45, No. 5, pp. 749–762, doi: 10.1016/j.ijrmms.2007.09.003.

KARAKUS D., ONUR A.H., DELIORMANLI A.H., and KONAK G., 2010, *Size and shape analysis of mineral particles using image processing technique*, Journal of Ore Dressing, Vol. 12, No. 23.

KAZHDAN M. and HOPPE H., 2013, *Screened poisson surface reconstruction, ACM Trans. Graph.*, Vol. 32, No. 3, Jun., doi: 10.1145/2487228.2487237.

KAZHDAN M., BOLITHO M., and HOPPE H., 2006, *Poisson Surface Reconstruction*, [in:] K. Polthier, A. Sheffer (Eds.), Eurographics Symposium on Geometry Processing.

KONER R. and CHAKRAVARTY D., 2016, *Characterisation of overburden dump materials: a case study from the Wardha valley coal field*, Bulletin of Engineering Geology and the Environment, Vol. 75, No. 3, pp. 1311–1323, Aug., doi: 10.1007/s10064-015-0830-x.

KONER R., 2021, *Estimation of Optimum Geometric Configuration of Mine Dumps in Wardha Valley Coalfields in India: A Case Study*, Journal of Mining and Environment, Vol. 12, No. 4, pp. 907–927, Sep., doi: 10.22044/jme.2021.10979.2074.

KWAN A.K.H., MORA C.F., and CHAN H.C., 1999, *Particle shape analysis of coarse aggregate using digital image processing, Cem. Concr. Res.*, Vol. 29, No. 9, pp. 1403–1410.

LIRA C. and PINA P., 2007, *Sedimentological analysis of sands*, [in:] *Lecture Notes in Computer Science (including subseries Lecture Notes in Artificial Intelligence and Lecture Notes in Bioinformatics)*, Springer-Verlag, pp. 388–396. doi: 10.1007/978-3-540-72849-8_49.

LU F., ZHOU X., and HE Y.B., 1988, *Image Segmentation Technique Used in Estimation of the Size Distribution of Rock Fragments in Mining, MVA*, pp. 351–354.

MAERZ N.H. and LUSHER M., 2001, *Measurement of flat and elongation of coarse aggregate using digital image processing*, [in:] *80th Annual Meeting, Transportation Research Board, Washington DC*, pp. 2–14. [Online]. Available: https://www.researchgate.net/publication/242107361

MAERZ N.H., 2004, *Technical and Computational Aspects of the Measurement of Aggregate Shape by Digital Image Analysis*, Journal of Computing in Civil Engineering, Vol. 18, No. 1, pp. 10–18, doi: 10.1061/ASCE0887-3801200418:110.

MIR B.A. and ASHRAF S., 2019, *Evaluation of load-settlement behaviour of square model footings resting on geogrid reinforced granular soils*, [in:] Advanced Research on Shallow Foundations, pp. 103–126, doi: 10.1007/978-3-030-01923-5.

MISHRA A., DAS S.K., and REDDY K.R., 2024, *Potential Use of Coal Mine Overburden Waste Rock as Sustainable Geomaterial: Review of Properties and Research Challenges*, J. Hazard Toxic Radioact. Waste, Vol. 28, No. 1, Jan., doi: 10.1061/jhtrbp.hzeng-1258.

MORA C.F. and KWAN A.K.H., 2000, *Sphericity, shape factor, and convexity measurement of coarse aggregate for concrete using digital image processing*, Cem. Concr. Res., Vol. 30, Issue 3, 351–358.

MORA C.F., KWAN A.K.H., and CHAN H.C., 1998, *Particle size distribution analysis of coarse aggregate using digital image processing*, Cem. Concr. Res., Vol. 28, No. 6, pp. 921–932.

NEUBECK A. and VAN GOOL L., 2006, *Efficient Non-Maximum Suppression*, ETH Zurich.

RUBIN D.M., 2004, *A Simple Autocorrelation Algorithm for Determining Grain Size from Digital Images of Sediment*," *JOURNAL OF SEDIMENTARY RESEARCH*, vol. 74, no. 1, pp. 160–165, [Online]. Available: http://pubs.geoscienceworld.org/sepm/jsedres/article-pdf/74/1/160/2819088/160.pdf

SERESHKI F., HOSEINI S.M., and ATAEI M., 2016, *Blast fragmentation analysis using image processing*, International Journal of Mining and Geo-Engineering, Vol. 50, No. 2, pp. 211–218, doi: 10.22059/ijmge.2016.59831.

TAYLOR M.A., 2002, *Quantitative measures for shape and size of particles*, Powder Technol., Vol. 124, No. 1–2, pp. 94–100. [Online]. Available: www.elsevier.com/locate/powtec

TRIGGS B., MCLAUCHLAN P., HARTLEY R., and FITZGIBBON A., 2000, *Bundle Adjustment – A Modern Synthesis*, Vision Algorithms: Theory and Practice: International Workshop on Vision Algorithms Corfu, Greece, pp. 298–372, doi: 10.1007/3-540-44480-7_21ï.

TUTUMLUER E., PAN T., and CARPENTER S.H., 2005. *Investigation of aggregate shape effects on hot mix performance using an image analysis approach, UILU-ENG*. [Online]. Available: http://www.pooledfund.org

VANGLA P., ROY N., MENDU K., and LATHA G.M., 2014, *Digital Image Analysis for the Determination of Size and Shape Parameters of Sand Grains*, [in:] *Golden Jubilee Conference of the IGS Bangalore Chapter, Geo Innovations, Bangalore India*. [Online]. Available: https://www.researchgate.net/publication/273261114